



HAL
open science

Absolute parameters and chemical composition of the binary star OU Gem

L. V. Glazunova, T. V. Mishenina, C. Soubiran, V. V. Kovtyukh

► **To cite this version:**

L. V. Glazunova, T. V. Mishenina, C. Soubiran, V. V. Kovtyukh. Absolute parameters and chemical composition of the binary star OU Gem. *Monthly Notices of the Royal Astronomical Society*, 2014, 444, pp.1901-1908. 10.1093/MNRAS/STU1576 . hal-01062039

HAL Id: hal-01062039

<https://hal.science/hal-01062039>

Submitted on 1 Dec 2021

HAL is a multi-disciplinary open access archive for the deposit and dissemination of scientific research documents, whether they are published or not. The documents may come from teaching and research institutions in France or abroad, or from public or private research centers.

L'archive ouverte pluridisciplinaire **HAL**, est destinée au dépôt et à la diffusion de documents scientifiques de niveau recherche, publiés ou non, émanant des établissements d'enseignement et de recherche français ou étrangers, des laboratoires publics ou privés.



Distributed under a Creative Commons Attribution 4.0 International License

Absolute parameters and chemical composition of the binary star OU Gem

L. V. Glazunova,^{1,2} T. V. Mishenina,^{1,3} C. Soubiran⁴ and V. V. Kovtyukh^{1,3★}

¹*Astronomical Observatory, Odessa National University, Shevchenko Park, Odessa 650014, Ukraine*

²*Odessa National Academy of Telecommunications, Kuznechnaya street 1, Odessa 65029, Ukraine*

³*Isaak Newton Institut of Chile, Odessa Branch, Shevchenko Park, Odessa 650014, Ukraine*

⁴*Université de Bordeaux – CNRS – Laboratoire d’Astrophysique de Bordeaux, UMR 5804, BP 89, F-33271 Floirac Cedex, France*

Accepted 2014 August 4. Received 2014 July 29; in original form 2014 February 19

ABSTRACT

The absolute parameters and chemical composition of the BY Dra-type spectroscopic binary OU Gem (HD 45088) were determined on the basis of 10 high-resolution spectra. A new orbital solution of the binary system was determined, the binary ephemerides were specified, and the main physical and atmospheric parameters of the binary components were obtained. The chemical composition of both components was estimated for the first time for the stars of such type.

Key words: stars: abundances – binaries: spectroscopic – stars: fundamental parameters – stars: individual: OU Gem.

1 INTRODUCTION

Spotted stars with marked chromospheric activity are quite common among stars in the lower part of the main sequence (MS). While studying the parameters and chemical composition of lower MS stars (Mishenina et al. 2008, 2012), we found more than 50 active stars. By applying the methods usually used for investigation of stars we did not observe any noticeable differences in the atmospheric parameters and chemical compositions of active and inactive stars, except those in their lithium abundances: a higher percentage of stars with lithium was detected among active stars. The complete chemical composition of active stars has rarely been investigated. For our new study we chose a complicated example from our investigated BY Dra-type stars (Mishenina et al. 2008), namely the spectroscopic binary OU Gem (HD 45088), to conduct the in-depth study of both its atmospheric parameters and chemical composition. On the one hand, the chemical composition of stars is an important parameter, which we can use to assess the relationship of a star with galactic structures and galactic chemical evolution, and, ultimately, to find out the star origin. On the other hand, the binary system study allows us for further verifying the binary parameters, clarifying its age (evolutionary status) and determination of the chemical composition of each component. The latter is also important with regard to the binary formation and origin.

The visual magnitude of OU Gem is $m_V = 6.77$ mag, its orbital period is $P = 6.99$ d. The two components are of close spectral types K3 V+K5 V. The binary is located at a distance of 14.73 pc

from *Hipparcos* (van Leeuwen 2007). The binary light curve does not exhibit eclipses, but shows a smooth variation in brightness with an amplitude in the range of 0.02–0.05 mag and period $P = 736$ d (Bopp et al. 1981) that is longer than the orbital one. The photometric light curve is typical for the BY Dra-type stars and it is likely to be associated with the spottiness of one of the binary components. The spectral orbital elements were determined by Tomkin (1980) and Griffin & Emerson (1975). In the study by Griffin & Emerson (1975), the spectral orbital elements were determined for the primary component only, but it was done with a large number of points on the radial velocity curve (54 points comparing to 12 points in Tomkin 1980). The binary orbit was found to have a high eccentricity ($e = 0.15$; e.g. Griffin & Emerson 1975), which can be indicative of the young age of the binary.

Strong emission in the Ca II H&K lines is observed in both components of OU Gem binary, as well as in many other BY Dra-type stars. The emission variation was studied by Montes et al. (1995, 2000). Accounting for the components contributions to the relative luminosity $L_A/L_B = 0.7/0.3$, the estimated equivalent widths of the components emission were 1.08/1.71 Å for the K line and 1.02/1.51 Å for the H line of the Ca II. As is seen from those estimations, the secondary component, which is less massive, has higher chromospheric activity. That is in good agreement with the dependence of the H&K lines equivalent widths on the stellar temperature and rotational velocity, observed in a large number of chromospherically active stars (Montes et al. 1996): the chromospheric activity grows with decreasing temperature and increasing rotational velocity. The equivalent width variation of the H α absorption lines for both binary components was also studied by Latorre, Montes & Fernández-Figueroa (2001). The equivalent width of the H α line

★E-mail: val@deneb1.odessa.ua

Table 1. The observation dates, new radial velocity and orbital phases.

JD 245 0000+	S/N	v_{rA} (km s ⁻¹)	σ	v_{rB} (km s ⁻¹)	σ	Phase
4898.313	71.2	43.17	0.6	-67.43	0.97	0.75
4899.293	173.4	45.71	0.9	-69.74	1.05	0.89
4900.280	133.4	-7.02	1.2	-	-	0.03
4901.395	123.0	-59.72	1.04	53.74	2.1	0.19
5128.695	126.5	32.22	0.5	-56.62	1.5	0.70
5130.627	156.8	17.25	0.9	-39.2	1.3	0.98
5131.623	136.4	-45.50	1.5	35.55	1.8	0.12
5132.622	161.9	-64.21	0.8	56.41	0.9	0.26
5835.685	88.9	49.65	0.5	-76.14	0.9	0.81
5836.684	87.0	25.50	0.5	-48.43	0.9	0.96

slightly change with the orbital phase for the primary component whilst the twofold change in the equivalent widths of the secondary component may be due to the H α emission line for that component.

In this work, we are focused on checking the binary system parameters and determination of the detailed chemical composition of its components.

2 OBSERVATIONAL MATERIAL

The spectral observations were conducted with the 1.93 m telescope equipped with the echelle-type spectrograph SOPHIE (Perruchot et al. 2008) at the Observatoire de Haute-Provence, France. The resolving power $R = 75\,000$ covers the wavelength range of 3870–6940 Å. The observation dates, signal-to-noise ratios (S/N) at the wavelength 5500 Å, heliocentric radial velocities v_{rA} and v_{rB} (A – the primary component, B – the secondary component), the accuracy in the radial velocity determination and new orbital phases are given in Table 1. The first eight spectra were obtained in 2009, and other two spectra in 2011.

The spectra processing, including the continuous spectrum level placement, the dispersion curve application, etc. was performed using the DECH20 software package (Galazutdinov 1992). The first version of the programme was created in 1992 by Galazutdinov (1992), the subsequent versions are available on website.¹ In general, the DECH20 software provides all stages of the CCD echelle-image-spectra processing: bias/background subtraction, flat-field division, one-dimensional spectrum extraction from two-dimensional images, correction for diffuse light, spectrum addition and exclusion of cosmic ray features. One can also carry out all types of spectra processing procedures and measurements: (1) removal of apparent defects in spectrum (manually); (2) smoothing the spectrum in different ways; (3) linearization; (4) spectrum fission for spectrum-star flat-field standard; (5) construction of the dispersion curve, including global polynomial spectral binding orders echelle spectrum; (6) set a continuum; (7) measurement of equivalent widths by different ways; and (8) measurement of radial velocities; etc. The DECH20 software can be used for a combined echelle spectrum, i.e. all echelle spectrum orders are consistently recorded in a single file.

The least-squares decomposed (LSD) profile method was applied to determine the components radial and rotational velocities ($v \sin i$). The first minimum of the Fourier transform of that profile allows for accurate estimation of the components rotational velocities. The method description and the programme testing results are given by Reiners & Royer (2004) and Glazunova et al. (2008). The VALD

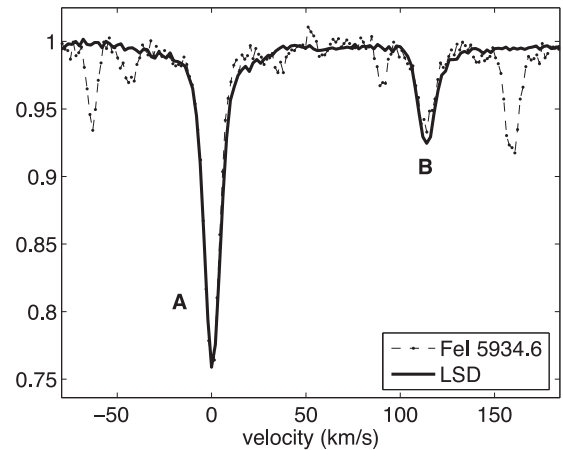


Figure 1. The LSD profile (solid line) and the observed spectrum (dashed line) in the region of Fe I λ 5934.6 Å line for OU Gem binary at the phase of 0.18.

list of lines (Piskunov et al. 1995) for the models with temperature 5000 and 4500 K was used for identification.

The projected rotational velocities of the OU Gem components $v_A \sin i$ and $v_B \sin i$ were obtained by LSD profile for each spectrum (see Table 3). The average projected rotational velocities of the components are 6.0 ± 0.3 km s⁻¹ for the primary component and 6.5 ± 0.6 km s⁻¹ for the secondary component. The OU Gem LSD profile and a portion of the observed spectrum are shown in Fig. 1.

The radial velocities of the components were calculated by averaging measurements of the LSD profile centroid and core. Table 2 presents the spectral orbital elements, which were obtained by our 10 spectra, and also the data from Tomkin (1980) and Griffin & Emerson (1975), as well as the simultaneous solution for all radial velocities. The orbital elements were derived by the standard procedure of ordinary least squares. As can be seen from Table 2, solutions by different authors are quite similar to each other, but the best result was achieved with the simultaneous solution for all radial velocities. The velocity curves for primary and secondary components are shown in Fig. 2.

3 DETERMINATION OF THE BINARY COMPONENTS TEMPERATURES

The components effective temperatures T_{eff} were determined by the ratio of intensities of lines with different excitation potential of a lower level. It was performed using the list of lines by Kovtyukh et al. (2003) that allowed for the high-accuracy determination of the

¹ <http://www.gazinur.com/DECH-software.html>

Table 2. New spectral orbital elements.

Elements	G&Em (component A)	Tomkin (components A+B)	Our data ($\sigma(v_{rA}) = 0.73, \sigma(v_{rB}) = 0.49$)	G&Em + Tomkin + ours ($\sigma(v_{rA}) = 1.31, \sigma(v_{rB}) = 1.27$)
P (d)	6.99187 ± 0.00007	6.9990 ± 0.003	6.99188 ± 0.000096	6.991878 ± 0.000004
T (d)	40203.163 ± 0.029	43867.020 ± 0.064	454900.144 ± 0.032	54900.0719 ± 0.0203
e	0.150 ± 0.004	0.141 ± 0.005	0.147 ± 0.005	0.151 ± 0.0024
ω ($^\circ$)	77.6 ± 1.4	81.4 ± 2.8	81.1 ± 1.8	77.63 ± 1.09
K_A	56.55 ± 0.21	55.97 ± 0.25	56.94 ± 0.31	57.09 ± 0.15
K_B		66.88 ± 0.19	66.64 ± 0.34	66.22 ± 0.28
γ	-8.40 ± 0.15	-10.37 ± 0.25	-8.23 ± 0.20	-8.98 ± 0.10
$M_A \sin^3 i (M_\odot)$		0.71	0.711 ± 0.005	0.705 ± 0.006
$M_B \sin^3 i (M_\odot)$		0.59	0.603 ± 0.004	0.608 ± 0.004
$asini$ (10^6 km)		12.68	11.68	12.59

Notes. G&Em – Griffin & Emerson (1975) and Tomkin – Tomkin (1980).

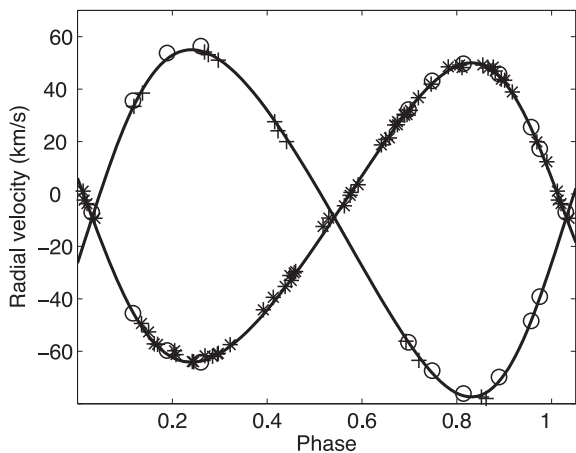


Figure 2. Orbital radial velocities of OU Gem binary: our data are marked with open circles, data by Griffin & Emerson (1975) – with asterisks, data by Tomkin (1980) – with crosses, the orbital solution – with solid line.

stellar temperatures in the range from 7000 to 4000 K. Temperatures for both binary components were estimated for each spectrum separately. To conduct such estimation, only those lines of the primary and secondary components, which were not blended in the spectra obtained at the given orbital phase, were selected from the list. The choice of non-blended lines for each component from this list was performed by comparing the observed and computed spectra with the `URAN` code (Yushchenko et al. 2004) based on the Kurucz models. The `URAN` code enabled us to compute the composite synthetic binary spectrum by its component parameters accounting for their contributions, line shift and broadening due to orbital motion and rotation, respectively, and then to compare it with the observed spectrum. The composite and observed spectra at the phase of 0.88 are shown in Fig. 3. The preliminary model parameters of the binary components were taken from Montes et al. (2000) and from Mishenina et al. (2009), and further refined.

The temperatures, ratios of relative luminosities and projected rotational velocities of the binary components determined at different orbital phases where the components lines are separated, as well as the orbital phase (for our new epoch of minimum $2454900.0719 + 6.9921 \cdot E$ d where E is the cycle number) are given in Table 3. The mean values for the indicated parameters are given in the last row of the table. The relative luminosities of the binary components were determined by the ratio of equivalent widths of the specially

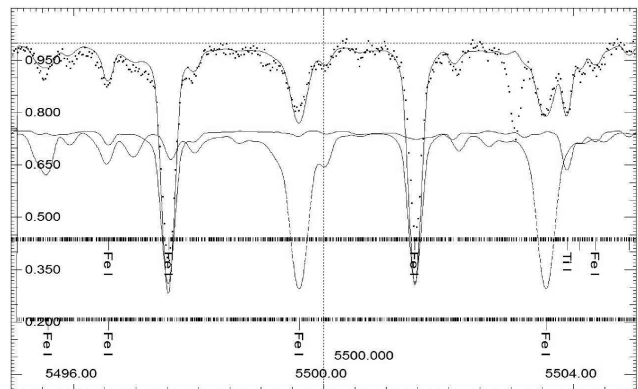


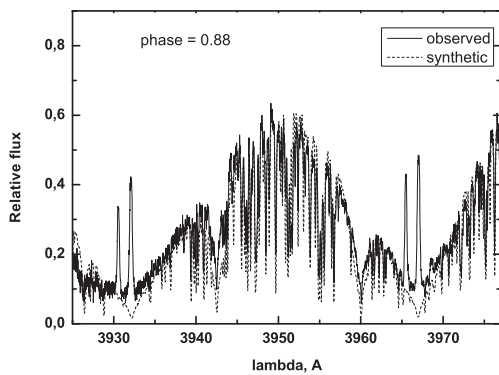
Figure 3. The `URAN` program screen: the OU Gem composite synthetic spectrum (solid line at the top) and observed spectrum at the phase of 0.88 (dotted line). The synthetic spectra for the primary (solid line) and secondary (dashed line) components are shown in the lower part. The positions of the spectral lines, which were accounted when calculating the synthetic spectra, are marked with short and long dashes (faint and strong lines). Some strong lines are identified.

selected components lines with almost similar intensity in the synthetic spectrum of each component.

As can be seen from Table 3, the primary component temperature is the same at all phases within the given accuracy, while the secondary component temperature tends to vary. The average temperature and accuracy for all spectra are given in Table 3. As can be seen from Table 3, the projected rotational velocities of the primary and secondary components were determined by the LSD profiles change for different spectrograms within $1\text{--}2 \text{ km s}^{-1}$; their mean value is higher than that one by Montes et al. (2000). Such a significant change in the rotational velocity for different binary spectra can be associated with the alteration of the line profile by the presence of spots on the components surfaces. As can be seen from Table 3, the relative luminosities also change ($\text{Fe}(L_A/L_B)$ – the relative luminosities are determined only by the iron lines, L_A/L_B are determined by other lines). Simultaneously, with the observations in 2009 when spectra (a), (b), (c) and (d) were obtained (see Table 1), the photometric observations were conducted by Mishenina et al. (2009); and it was reported that at the moment of the (d) spectrum observation the $B - V$ colour index of the binary was 0.02 mag lower than that one at the moment of (a) spectrum observation, i.e. the colour index was maximum at the phases of spectra (a), (b) and (c); thus, the secondary component contribution to the total spectrum increased. Spectrum (a) confirms the above conclusion,

Table 3. The temperatures, relative luminosities and projected rotational velocities of the components for all spectra (a, b, c and d point out the availability of photometric data for corresponding JD)

JD 245 0000+	$T_{\text{eff}A}$	$T_{\text{eff}B}$	Fe(L_A/L_B)	L_A/L_B	$v_A \sin i$	$v_B \sin i$	Phase
4898.313(a)	5044 ± 22	4693 ± 134	0.74/0.26	0.71/0.29	6.14	6.57	0.75
4899.293(b)	5013 ± 15	4486 ± 107	0.78/0.22	0.74/0.26	5.2	5.30	0.89
4900.280(c)	4881						0.03
4901.395(d)	5025 ± 10	4538 ± 58	0.75/0.25	0.74/0.26	6.17	6.94	0.19
5128.695	5027 ± 13	4559 ± 163	0.73/0.27	0.72/0.28	5.94	6.53	0.70
5130.627	4985 ± 13	4275 ± 96	0.75/0.25	0.73/0.27	5.97	6.14	0.98
5131.623	5036 ± 12	4498 ± 149	0.76/0.24	0.74/0.26	5.89	6.29	0.12
5132.622	5058 ± 10	4578 ± 113	0.76/0.24	0.74/0.26	5.93	6.24	0.26
5835.685	5027 ± 14	4459 ± 135	0.78/0.22	0.70/0.30	5.94	6.93	0.81
5836.684	5010 ± 11	4484 ± 30	0.72/0.28	0.71/0.29	6.48	7.43	0.96
Average	5025 ± 13	4508 ± 105	0.75 ± 0.03/0.25	0.73/0.27	5.96 ± 0.3	6.49 ± 0.6	

**Figure 4.** The H&K Ca II emission lines for the primary and secondary components at the phase of 0.88. (Note that the emission of the secondary is larger after the corruption from the contribution of each component to the total continuum.)

but spectrum (b) does not although their orbital phases are close. It can be an indication of the fact that variations in the secondary component temperature and relative luminosity contributions by the components (see Table 3) do not reflect reality.

4 DETERMINATION OF THE BINARY COMPONENTS' ABSOLUTE PARAMETERS

Taking into account that the H&K Ca II emission lines are stronger for the secondary component in the subtracted spectra of each component, and the H_α line of that component shows a considerable variation, it is possible to conclude that the secondary component is more chromospherically active and responsible for the binary brightness variation (see Fig. 4 and Montes et al. 1995, 2000). That allows us to estimate the minimum radius of the secondary component by its known rotation period $P = 7.36$ d (provided that the binary brightness varies due to the spots on the secondary component surface), as well as the projected linear rotational velocity for $v \sin i = 6.5 \text{ km s}^{-1}$ and $i = 90^\circ$:

$$R_B = \frac{vP}{2\pi \sin i} = 0.95 R_\odot. \quad (1)$$

Such a radius for the MS stars can correspond to a star with mass of about $1 M_\odot$ (Zahn 1994), and thus, if the spots on the surface are located near the equator, the orbital inclination to the plane of projection i should be around 58° . However, those spots can be

located far from the equator, so as a result of differential rotation of such star, the rotational velocity should decrease. This is a possible reason for the photometric period being longer than the spectral orbital period obtained by the radial velocity curve.

It is possible to determine the components radii and, consequently, the orbital inclination to the plane of projection by estimating the components luminosities. To determine the absolute magnitude of the binary, we used the binary parallax value of $68.2 \pm 1.1 \text{ mas}$ from *Hipparcos* (van Leeuwen 2007), which corresponds to the distance $d = 14.73 \pm 0.33 \text{ pc}$. That distance makes it possible to neglect the interstellar absorption; then, the absolute magnitude through filter V is $M_V = m_V + 5 - 5 \cdot \log d = 5.93 \text{ mag}$. Then, the binary luminosity in the V band equals to $\log L/L_\odot = -0.440 \pm 0.002$ ($L = 0.363 \pm 0.014 L_\odot$). Accounting for the luminosity contribution for the V band (see Table 3) of 0.75 ($\log L_A/L_\odot = -0.565$) by the primary component and 0.25 ($\log L_B/L_\odot = -1.042$) by the secondary component, it is possible to determine the components absolute magnitudes in the V band: $M_{VA} = 6.24 \pm 0.10 \text{ mag}$, $M_{VB} = 7.44 \pm 0.10 \text{ mag}$. The components temperatures, their absolute magnitudes in the V band and metallicities, as well as the binary age enable to determine the components mass by the evolutionary tracks.

Therefore, the primary component mass should be $0.78 \pm 0.02 M_\odot$ with $i = 74^\circ 7 \pm 3$, and the secondary component mass should be $0.66 \pm 0.02 M_\odot$ with $i = 75^\circ 6 \pm 3$ used for determination of the evolutionary tracks for the stars with mass of $0.6\text{--}1.0 M_\odot$, metallicities $[\text{Fe}/\text{H}] = -0.25$ and $[\text{Fe}/\text{H}] = 0.06$ for the age of $10^{8.5}$ years by Pietrinferni et al. (2006) (see Fig. 5). Although the binary components are located near the evolutionary track with $[\text{Fe}/\text{H}] = 0.06$, we determined the mass by the evolutionary track with $[\text{Fe}/\text{H}] = -0.25$ as appropriate for the components metallicity (the linear interpolation by M_V) and $\log T_{\text{eff}}$, as well as the accuracy in determination of M_V and T_{eff} . The error was estimated by the accuracy of the components relative luminosities and distance. Having made the bolometric correction $BC_A = -0.295 \text{ mag}$ for $T_{\text{eff}} = 5025 \text{ K}$ ($\log T_{\text{eff}} = 3.70 \pm 0.002$) and $BC_B = -0.525 \text{ mag}$ for $T_{\text{eff}} = 4508 \text{ K}$ ($\log T_{\text{eff}} = 3.65 \pm 0.014$), obtained by the calibration by Flower (1996), we got the absolute bolometric magnitudes for the components $M_{\text{bol}A} = 5.95 \text{ mag}$, $M_{\text{bol}B} = 6.91 \text{ mag}$ and the components radii $R_A = 0.79 \pm 0.04 R_\odot$ and $R_B = 0.63 \pm 0.05 R_\odot$. So the orbital inclination can be asserted equal to $i = 75^\circ 2 \pm 3$ that it is in good correspondence with the absence of eclipses in the binary, which could occur for those components radii if $i > 83^\circ$. The evolutionary tracks of the stars with mass of $0.6\text{--}0.8 M_\odot$ and

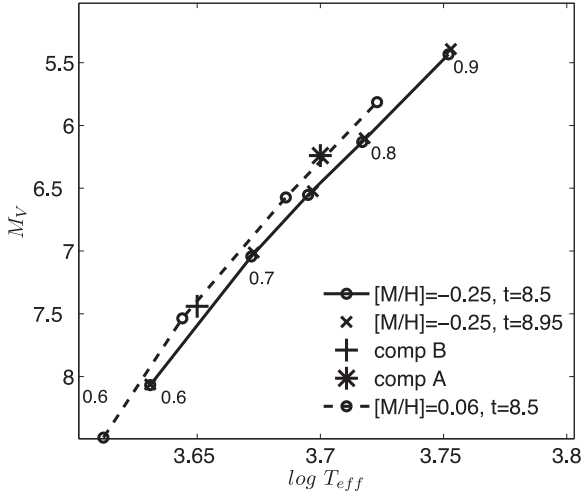


Figure 5. The positions of the binary components and evolutionary tracks of the stars with mass of 0.6, 0.7, 0.75, 0.8 and metallicity $[\text{Fe}/\text{H}] = -0.25$ (solid lines) and $[\text{Fe}/\text{H}] = 0.06$ (dashed lines) for the age of $10^{8.5}$ years (for comparison, also the tracks for the age of $10^{8.95}$ are marked by crosses) by Pietrinferni et al. (2006).

metallicities $[\text{Fe}/\text{H}] = -0.25$ and $[\text{Fe}/\text{H}] = 0.06$ for the age $10^{8.5}$ years, for comparison, also we give the tracks for the age of $10^{8.95}$ years as well as the positions of the binary components are presented in Fig. 5.

Thus, based on the spectral elements of the orbits, the luminosities of the binary components, determined by the known parallax and their contributions to the composite spectrum estimated by the line depth ratio, we computed the absolute parameters of the binary components (see Table 4).

5 THE ATMOSPHERIC MODEL PARAMETERS OF THE OU GEM COMPONENTS

According to the results of the depth ratio study for the selected lines, the temperatures for the primary and secondary components were assumed to be 5025 and 4508 K, respectively. Earlier, on the basis of estimated masses and radii of the binary components we determined that the surface gravity was 4.53 and 4.66 for the primary and secondary components, respectively. However, assuming the ionization equilibrium for the iron atoms, the surface gravity should be equal to 4.3 and 4.5 for the primary and secondary components, respectively. So, the difference in the determination of the components' surface gravities by those methods is equal to 0.2. Such a discrepancy in determination of the gravity values by different methods for the late-type stars was investigated by Tsantaki et al. (2013). The authors reported that the difference in determination of the surface gravity by spectral lines, as well as known

Table 4. The absolute parameters of the binary components.

Parameters	Comp. A	Comp. B
$\log L/L_{\odot}$	-0.447 ± 0.04	-0.832 ± 0.04
$M(M_{\odot})$	0.78 ± 0.02	0.66
$R(R_{\odot})$	0.79 ± 0.04	0.63 ± 0.05
$\log g$	4.53 ± 0.06	4.66 ± 0.08

Table 5. The atmospheric parameters.

Parameters	Comp. A	Comp. B
$T_{\text{eff}} (K)$	5025	4508
$\log g$	4.3	4.5
$\xi (\text{km s}^{-1})$	1.3	1.5
L_{rel}	0.78	0.22

masses and radii for the stars with temperature of 5000 K is 0.2 (in the logarithmic scale) that is close to our results.

The microturbulent velocities ξ were determined under the condition that the iron abundance estimated by the line is independent from its equivalent width, and they are equal to 1.3 and 1.5 km s^{-1} for the primary and secondary components, respectively.

For improvement, the parameters of stellar atmospheres with a help models of the atmospheres we used the method of interpolation process: first, the temperature was determined, then $\log g$, ξ . Further with the obtained values ξ we re-determine $\log g$, ξ , etc. until we got the values with the given accuracy (0.03 for $\log g$, ξ), and eventually we determine the final values $\log g$, ξ and $[\text{Fe}/\text{H}]$. To compute the composite spectrum of the binary, it is necessary to know the contributions by its components. The best way to determine the components contributions is to analyse eclipses. However, the high-precision photometry (0.01 mag) of the binary by Tomkin (1980) did not show presence of any eclipses. So the components contributions can be theoretically calculated using the ratio of radiation fluxes from continuous spectra of the components, which were obtained by the above-indicated parameters of their atmospheres (see Table 4). Applying that method gives the flux ratio at the wavelength 5500 Å equal to $F_A/F_B = 1.93$, and therefore, the components relative luminosities near 5500 Å are $L_A = 0.71$ and $L_B = 0.29$ ($L_A/L_B = (F_A \cdot R_A^2)/(F_B \cdot R_B^2)$) and $L_A + L_B = 1$). Another way to estimate the components contributions into the composite spectra in accordance with a formula by Lyubimkov (1995) is to analyse the equivalent width ratio of the lines with the same intensity in the spectra of the primary and secondary components:

$$r_{\lambda}(A) = r_{\lambda}^{\text{obs}} \times (1 + \beta_{\lambda}); \beta_{\lambda} = \frac{F_{\lambda}(B)}{F_{\lambda}(A)} \times \left(\frac{R_B}{R_A}\right)^2, \quad (2)$$

where $r_{\lambda}(A)$ is a line depth of the A component. For calculation, $r_{\lambda}(B)$ uses $\beta_{\lambda} = \frac{F_{\lambda}(A)}{F_{\lambda}(B)} \times \left(\frac{R_A}{R_B}\right)^2$. To eliminate the effects of the temperature on the line depth, we selected 15 iron lines within the range of 5500–6000 Å, which have almost similar intensities in the synthetic spectra of those components and because the difference of the equivalent widths of the lines in the composite spectra will depend only on the components relative luminosities; and the components contributions into the binary luminosity were determined by those lines as $L_A/L_B = 3$; therefore, $L_A = 0.75 \pm 0.03$ and $L_B = 0.25$ (see Table 3). However, it is only relative luminosities of the components $L_A = 0.78$ and $L_B = 0.22$ that allow us to get almost similar iron abundances in their atmospheres; while the luminosities obtained on the basis of the atmospheric models ($L_A = 0.71$ and $L_B = 0.29$) lead to a considerable difference in the iron abundance in the components atmospheres, and that is rather difficult to explain in the context of the binary evolution.

The final parameters of the atmospheric models of the binary components required to compute the composite synthetic spectrum are given in Table 5.

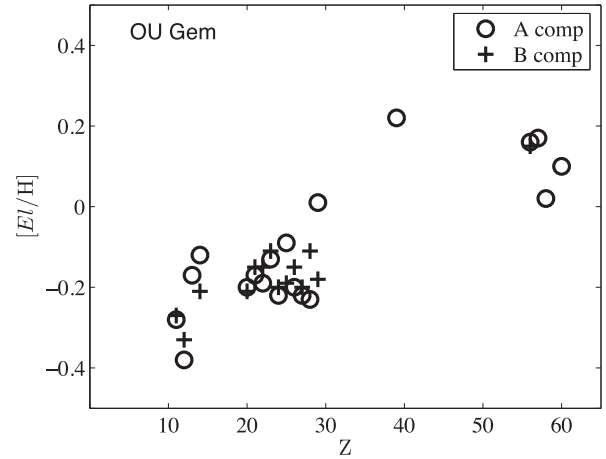
Table 6. The elemental abundances in the binary components.

Element (Z)	A comp.		B comp.	
	[El/H](σ)	N lines	[El/H](σ)	N lines
Na(11)	-0.28(0.11)	7	-0.27(0.33)	3
Mg(12)	-0.38(0.15)	5	-0.33(0.18)	2
Al(13)	-0.17(0.15)	2		
Si(14)	-0.12(0.08)	28	-0.21(0.17)	5
Ca(20)	-0.20(0.08)	19	-0.21(0.22)	4
Sc(21)	-0.17(0.08)	23	-0.15(0.24)	4
Ti(22)	-0.19(0.09)	78	-0.15(0.12)	44
V(23)	-0.13(0.12)	43	-0.11(0.04)	7
Cr(24)	-0.22(0.12)	34	-0.20(0.10)	13
Mn(25)	-0.09(0.19)	10	-0.19(0.21)	3
Fe(26)	-0.20(0.10)	475	-0.15(0.19)	176
Co(27)	-0.22(0.12)	24	-0.20(0.12)	3
Ni(28)	-0.23(0.12)	91	-0.11(0.12)	34
Cu(29)	0.01(0.05)	3	-0.18(0.20)	1
Y(39)	0.22(0.03)	3		
Ba(56)	0.16(0.05)	5	0.15(0.07)	3
La(57)	0.17(0.07)	3		
Ce(58)	0.02(0.03)	2		
Nd(60)	0.10(0.02)	2		

6 THE CHEMICAL COMPOSITION OF THE OU GEM COMPONENTS

Using the `URAN` code, the non-blended lines of the primary and secondary components were identified in the spectra at different phases of the orbital period. Their equivalent widths were measured and subsequently parted accounting for the change in the contribution of each component at different wavelengths according to the ratio of radiation flux of the components $L_A = 0.78$ and $L_B = 0.22$. The abundances of different chemical elements in the atmospheres of the binary components were determined by the reconstructed equivalent widths. The chemical composition was determined using two spectra with the highest S/N, as such spectra (b) and (d). The number of used lines of the primary and secondary components are given in Table 6 from two spectra (b, d) together. We used 459 Fe I lines and 16 Fe II lines for A component and 176 Fe I lines for B component. The list of used lines is given in Table 7 and available online.

To compute the elemental abundances we apply the grid of stellar atmospheres by Kurucz (1993). The choice of the model was made by the standard interpolation on T_{eff} and $\log g$. The abundance analysis has been conducted in the local thermodynamic equilibrium (LTE) approximation (with the Kurucz's `WIDTH9` code) using the measured equivalent widths of those elements lines and the solar

**Figure 6.** The relative abundances of chemical elements in the atmospheres of the OU Gem binary components according to their atomic numbers.

oscillator strengths (Kovtyukh & Andrievsky 1999). The influence of the non-local thermodynamic equilibrium (NLTE) effects on the barium lines is insignificant in the examined stars; the NLTE corrections for the barium abundances do not exceed 0.1 dex. The abundances of various chemical elements in the atmospheres of the binary components relative to those of the Sun are calculated as an average of two OU Gem spectra and shown in Fig. 6 and Table 6.

The abundances of 19 elements were estimated in the primary component spectrum (with an accuracy of 0.10 dex for the iron lines), and those of 14 elements were estimated in the spectrum of the secondary component (with an accuracy of 0.19 dex for the iron lines). As is seen in Fig. 6, the chemical composition of the primary and secondary components are in close agreement within the determination errors. There is a slight deficiency in metals ($[\text{Fe}/\text{H}] = -0.2$ dex) in the binary components relative to those solar ones. However, heavy elements, such as Y(39), Ba(56), La(57) and Nd(60) are overabundant relative to iron. Three intense lines in the spectra of both the primary and secondary components were used to determine the barium abundance; but unfortunately, those lines were affected by the NLTE departures. The abundance estimates for heavy elements, such as lanthanum and neodymium, were based on just one or two lines that might result in low accuracy. Taking into account the above, it can be concluded that there is only probable overabundance of the neutron-capture elements with respect to their solar abundances.

Table 7. Line parameters, equivalent widths of lines and abundances (only header of the table is shown. The full table is available in electronic form).

Element	λ (\AA)	$\log gf$	EPL (eV)	EW, m \AA	EW, m \AA	EW, m \AA	EW, m \AA	(El/H)	(El/H)	(El/H)	(El/H)
				(A comp)	(B comp)	(A comp)	(B comp)	(A comp)	(B comp)	(A comp)	(B comp)
				Sp 'd'	Sp 'd'	Sp 'b'	Sp 'b'	Sp 'd'	Sp 'd'	Sp 'b'	Sp 'b'
C I	5380.34	-1.84	7.68			17.1				9.029	
Na I	5682.65	-0.52	2.10	135.5	163.0	117.1		6.028	5.720	5.833	
Na I	5688.22	-0.45	2.10	181.4				6.338		6.232	
Na I	6154.23	-1.54	2.10	57.9	111.2	58.3		6.093	6.289	6.098	
Na I	6160.75	-1.22	2.10	80.9	67.5		137.4	6.078	5.494	5.970	6.191
Mg I	5528.42	-0.62	4.34	299.8		316.5		7.593		7.649	
Mg I	5711.09	-1.83	4.34	151.9	135.8	133.4		7.678	7.378	7.513	
Mg I	6318.71	-1.73	5.11	48.8	44.3	46.0		7.142	7.123	7.100	
Mg I	6319.24	-1.95	5.11	32.3		34.8		7.096		7.141	

7 RESULTS AND DISCUSSION

According to Bopp & Fekel (1977) who discovered the BY Dra-type binaries, such binary systems are those composed of K and M dwarf components, which exhibit low-amplitude variation in their light curves within a period of several days and have the Ca II H&K lines emission. As of today, there are about 41 known binaries of this type (Eker et al. 2008). The study of such binaries has been focused mainly on searching the photometric variability and the emission variation in the Ca II H&K and H α lines, associated with the chromospheric activity of the binary components. The most thorough studies are aimed to determine the dimensions and location of the spots on the stellar surface by changes in the line profiles with the photometric and orbital phase (Helminiak et al. 2012), as well as to pick out the emission profile from the binary composite line profile and estimate the energy flux of the emitted radiation.

Having analysed 10 high-resolution spectra of OU Gem binary, we obtained new spectral elements of the components orbits and more accurately estimated the binary spectral ephemerides, as well as the main parameters of the binary components and their atmospheres. The chemical composition of both components atmospheres was estimated for the first time for the stars of this type.

The pseudo-synchronous velocities of the binary components were calculated using the equation by Giuricin, Mardirossian & Mezzetti (1984):

$$v_{\text{ps}} = v_{\text{circle}}(1 + e)^{1/2}/(1 - e)^{3/2}, \quad (3)$$

where $v_{\text{circle}} = 2\pi R_*/P_{\text{sp}}$, R_* is the star radius, $P_{\text{sp}} = 6.9921$ d. Those velocities are 8.0 ($v_{\text{ps}} \sin i = 7.7 \text{ km s}^{-1}$) and 5.7 ($v_{\text{ps}} \sin i = 5.6 \text{ km s}^{-1}$) (the radii are taken from Table 4, $i = 75^\circ$).

The observed rotational velocity (see Table 3) of the primary component is 28 per cent slower than its pseudo-synchronous one; and the rotational velocity of the secondary component is 14 per cent higher; thus, accounting for the pseudo-synchronous velocity estimates obtained by the components masses, it can be suggested that the secondary component rotational velocity is similar to the synchronous velocity ($<3\sigma$), and the primary components rotational velocity is likely to be slower than the pseudo-synchronous one ($>3\sigma$).

The synchronization and circularization time for the binary components were calculated with the formula by Devor et al. (2008) for the stars with masses less than $1.3 M_\odot$:

$$t_{\text{syn}} \approx 0.00672 \left(\frac{k_2}{0.005} \right)^{-1} q^{-2} (1+q)^2 P^4 \left(\frac{M}{M_\odot} \right)^{-4.82} \quad (4)$$

where k_2 is taken from the paper by Zahn (1994), t_{syn} is given in Myr and P is given in days; hence, the synchronization and circularization is $t_{\text{synA}} = 130$ Myr, $t_{\text{synB}} = 240$ Myr, $t_{\text{cirA}} = 30$ Gyr (Zahn 1977).

The fact that the primary component is slightly asynchronous can be indicative of the binary age of about 100 Myr. Earlier OU Gem binary was considered to be a candidate member of the UMa group of the stars with the age of 300 Myr (Montes et al. 2000). However, the in-depth study by King et al. (2003), showed that OU Gem does not belong to the UMa group by its kinematic criteria albeit its spatial velocities correspond to those of young stars in the Sun vicinity (Eggen 1989).

High chromospheric activity of the binary components can also indicate that the binary is relatively young. The binary age can be estimated by the total flux in the Ca II H&K emission lines.

That value is conditioned by parameter $\log R'_{\text{HK}}$, which is equal to -4.39 and -4.50 for the primary and secondary components, respectively (according to the data by Montes et al. 2000). Using the approximation formula from the paper by Mamajec & Hillenbrand (2008), it is possible to determine that the estimated median age of the binary components is 450 ± 150 Myr that is close to the age of the UMa group (500 Myr according to the estimates by King et al. 2003). On the other hand, higher chromospheric activity of the binary can be resulted from binarity that increases the rotational velocity with a short period of rotation owing to tidal interaction as it is observed in the RS CVn stars. It might be the reason of high chromospheric activity of stars of the BY Dra system, which is estimated to be 1–2 Gyr of age and located between the Galactic thick and thin discs (Helminiak et al. 2012). Using the formula by Mamajec & Hillenbrand (2008) for estimation of the binary age by the periods of rotation of its components (gyrochronology), we obtained the age of 40–250 Myr. The positions of the OU Gem components in the evolutionary track diagram of stars with masses $0.6\text{--}0.9 M_\odot$ (see Fig. 5) do not contradict the above estimates of age. Therefore, it can be suggested that the binary age is about 250 ± 200 Myr.

The obtained metallicity in the OU Gem binary components atmospheres is $[\text{Fe}/\text{H}] = -0.20 \pm 0.10$ dex, and that is lower than the average metallicity in the atmospheres of the UMa group members, which is $[\text{Fe}/\text{H}] = -0.03 \pm 0.05$ dex (Ammler-von Eiff & Guenther 2009) and $[\text{Fe}/\text{H}] = 0.01 \pm 0.03$ dex (Biazzo et al. 2012). This also supports the conclusion that OU Gem binary does not belong to the UMa group. It is possible to notice a slight trend on the distribution of abundances of chemical elements by their atomic numbers (Fig. 6), which was determined by us for both binary components, i.e. one can observe the increasing of elemental abundances relative to the solar ones with increasing atomic numbers. Both components practically demonstrate similar dependences of chemical elements abundances on their atomic numbers.

We detected a noticeable deficiency in magnesium and overabundance of elements, generated during the neutron-capture processes. The analysis of chemical composition of atmospheres of stars with high chromospheric activity, like the RS CVn stars, shows marked deviation of elemental distribution comparing to normal G–K stars of IV–III luminosity classes (Bariševicius et al. 2010; Tautvaišienė et al. 2010).

A large deviation in abundances of some elements, determined by different researchers in the atmosphere of one and the same star, can be observed. That can be associated with the presence of large spots on the active star's surface where the temperature can be lower by 1000–2000 K than the photospheric one, and apparent area of which changes with time due to the star rotation (Bariševicius et al. 2010), as well as with the presence of gas and dust envelopes in those binaries (Kang et al. 2013).

Of note, interesting results were obtained when studying the chemical composition of the components of the RS CVn type LX Per binary (Kang et al. 2013), which contains an active K giant with a spot of 1000 K lower temperature than its photosphere and a G dwarf. Underabundances of heavy elements in the atmospheres of both binary components was detected by authors of this paper.

Thus, although the BY Dra-type OU Gem binary is at a different evolutionary stage than the RS CVn binaries, its high chromospheric activity may also cause some peculiarity of chemical compositions of its components, which generally depend on a number of other factors. To verify the peculiarity of the OU Gem chemical composition obtained by us, further in-depth chemical abundance

study of the BY Dra-type stars, both binaries and single stars, is needed.

ACKNOWLEDGEMENTS

This work is based on spectra collected with the 1.93 m telescope of the OHP (France). The authors are grateful to the Swiss National Science Foundation for their kind support under project SCOPES no. IZ73Z0_152485. We thank very much the anonymous referee for the useful suggestions that noticeably improved our manuscript.

REFERENCES

- Ammler-von Eiff M., Guenther E. D., 2009, *A&A*, 508, 677
- Barisevičius G., Tautvaišiene G., Berdyugina S., Chorniy Y., Ilyin I., 2010, *Balt. Astron.*, 19, 157
- Biazzo K., D'Orazi V., Desidera S., Covino E., Alcal J. M., Zusi M., 2012, *MNRAS*, 427, 2905
- Bopp B. W., Douglas S. H., Gregory W. H., Noah P., Klimke A., 1981, *PASP*, 93, 504
- Bopp B. W., Fekel F. C., 1977, *AJ*, 276, 345
- Devor J. et al., 2008, *ApJ*, 687, 1253
- Eggen O., 1989, *PASP*, 101, 366
- Eker Z. et al., 2008, *MNRAS*, 389, 1722
- Flower P. J., 1996, *ApJ*, 469, 355
- Galazutdinov G. A., 1992, *SAO RAS*, n92, preprint
- Giuricin G., Mardirossian F., Mezzetti M., 1984, *A&A*, 135, 393
- Glazunova L. V., Yushchenko A. V., Tsymbal V. V., Mkrichian D. E., Lee J. J., Kang Y. W., Valyavin G. G., Lee B.-C., 2008, *AJ*, 136, 1736
- Griffin R. F., Emerson B., 1975, *Observatory*, 95, 23
- Helminiak K. G., Konacki M., Muterspaugh M. W., Browne S. E., Howard A. W., Kulkarni S. R., 2012, *MNRAS*, 419, 1285
- Kang Y.-W., Yushchenko A. V., Hong K., Guinan E. F., Gopka V. F., 2013, *AJ*, 145, 167
- King J. R., Villarreal A. R., Soderblom D. R., Gulliver A. F., Adelman S. J., 2003, *AJ*, 125, 1980
- Kovtyukh V. V., Andrievsky S. M., 1999, *A&A*, 351, 597
- Kovtyukh V. V., Soubiran C., Belik S. I., Gorlova N. I., 2003, *A&A*, 411, 559
- Kurucz R. L., 1993, CD ROM n13
- Latorre A., Montes D., Fernández-Figueroa M. J., 2001, in Garcia Lopez R. J., Reboło R., Zapatero Osorio M. R., eds, *ASP Conf. Ser. Vol. 223, Multiwavelength Optical Observations of Chromospherically Active Binary System OU Gem. Astron. Soc. Pac., San Francisco*, p. 997
- Lyubimkov L. S., 1995, *Chemical Composition of Stars: Method and Results of Analysis*. Astroprint, Odessa
- Mamajek E. E., Hillenbrand L. A., 2008, *ApJ*, 687, 1264
- Mishenina T. V., Soubiran C., Bienayme O., Korotin S. A., Belik S. I., Usenko I. A., Kovtyukh V. V., 2008, *A&A*, 489, 923
- Mishenina T. V., Soubiran C., Kovtyukh V. V., Dubovsky P. A., Kudzej I., 2009, *Kinematika Fiz. Nebesnykh Tel.*, 26, 333
- Mishenina T. V., Soubiran C., Kovtyukh V. V., Katsova M. M., Livshits M. A., 2012, *A&A*, 547, 8
- Montes D., De Castro E., Fernández-Figueroa M. J., Cornide M., 1995, *A&AS*, 114, 287
- Montes D., Fernández-Figueroa M. J., Cornide M., De Castro E., 1996, *A&A*, 312, 221
- Montes D., Fernández-Figueroa M. J., De Castro E., Cornide M., Latorre A., Sanz-Forcada J., 2000, *A&AS*, 146, 103
- Perruchot S. et al., 2008, *Proc. SPIE*, 7014, 70140J
- Pietrinfermi A., Cassisi S., Salaris M., Castelli F., 2006, *ApJ*, 642, 797
- Piskunov N., Kupka F., Ryabchikova T., Weiss W., Jeffery C., 1995, *A&AS*, 112, 525
- Reiners A., Royer F., 2004, *A&A*, 428, 199
- Tautvaišiene G., Barisevičius G., Berdyugina S., Chorniy Y., Ilyin I., 2010, *Balt. Astron.*, 19, 95
- Tomkin J., 1980, *AJ*, 85, 294
- Tsantaki M., Sousa S. G., Adibekyan V. Zh., Santos N. S., Mortier A., Israelian G., 2013, *A&A*, 555, 150
- van Leeuwen F., 2007, *A&A*, 474, 653
- Yushchenko A. V., Gopka V. F., Khokhlova V. L., Lambert D. L., Kim C., Kang Y. W., 2004, *A&A*, 425, 171
- Zahn J. P., 1977, *A&A*, 57, 383
- Zahn J. P., 1994, *A&A*, 288, 829

SUPPORTING INFORMATION

Additional Supporting Information may be found in the online version of this article:

Table 7. Line parameters, equivalent widths of lines and abundances. (<http://mnras.oxfordjournals.org/lookup/suppl/doi:10.1093/mnras/stu1576/-/DC1>).

Please note: Oxford University Press are not responsible for the content or functionality of any supporting materials supplied by the authors. Any queries (other than missing material) should be directed to the corresponding author for the paper.

This paper has been typeset from a $\text{\TeX}/\text{\LaTeX}$ file prepared by the author.